

JOINT INSTITUTE FOR NUCLEAR RESEARCH

Dzhelepov Laboratory of Nuclear Problems

## FINAL REPORT ON THE SUMMER STUDENT PROGRAM

*Definition of the effective area of a neutrino  
telescope NT-1000 cluster*

**Supervisor:**

Dr. Bair Alexandrovich Shaybonov

**Student:**

Radik Rafaelevich Nugmanov

**Participation period:**

July 08 - August 25

Dubna, 2018

# Contents

<b>1</b>	<b>Abstract</b>	<b>2</b>
<b>2</b>	<b>Introduction</b>	<b>2</b>
2.1	The idea of neutrino registration . . . . .	2
2.2	Underwater neutrino telescopes NT-1000 . . . . .	3
<b>3</b>	<b>Analysis of the data obtained by Monte Carlo</b>	<b>3</b>
3.1	Angular and energy distribution of events . . . . .	4
3.2	Triggered strings distribution with separation on energy intervals and without . . . . .	4
3.3	Zenith angle cosine distribution for $6 \geq 2$ , $6 \geq 3$ and all events with energy separation and percentage ratio . . . . .	6
<b>4</b>	<b>Analysis of NT-1000 cluster transparency for low-energy muons</b>	<b>7</b>
4.1	Search for insensitive zones candidates . . . . .	7
4.2	Coordinates transformation . . . . .	9
<b>5</b>	<b>Effective and geometrical areas of a NT-1000 cluster</b>	<b>10</b>
5.1	Geometrical projection . . . . .	10
5.2	Calculation of effective areas . . . . .	11
<b>6</b>	<b>Conclusion</b>	<b>14</b>

# 1 Abstract

The effective area is an important characteristic of all neutrino telescopes. It shows how much neutrino this detector can register in a unit of time. This paper is devoted to the definition of the effective area of the cluster of neutrino telescope NT-1000. Data obtained by the Monte Carlo method were used to determine the effective area. These data were used to plot the dependence of the absolute effective area on the energy of the incident particles and on the Zenith angle of incidence of muons on the telescope. Since the natural noise of the detector is about 20 kHz, a noise filter has been applied to these events. After this was applied the algorithm for the reconstruction of the track of a muon that passed through the detector. The algorithm recovers tracks of not all muons flying through the detector, so the effective area of the detector will be reduced after applying the muon track reconstruction algorithm. As a result, this paper presents the effective area at each step of the application of different cuts and triggers.

## 2 Introduction

### 2.1 The idea of neutrino registration

In 1960, M. Markov, a Soviet theoretical physicist who has done a lot of work in the field of neutrino physics, has justified the possibility of observing neutrinos in underground observatories. He proposed to register neutrinos in lakes and oceans – deep under water. This is possible through the so-called Cherenkov radiation. The fact is that the speed of light when passing through water falls somewhat due to the interaction of photons with water. At the same time, neutrino, as a result of small interactions with water, generates a set of charged particles that have high energy and move through water faster than photons – that is, than light that moves in water.

In the case where a charged particle moves through a transparent medium at a speed greater than the speed of light in this medium – it emits a large number of photons that can be registered. This phenomenon is called-the effect of Vavilov-Cherenkov.

Thus, neutrinos flying through the water, when interacting with the medium, emit charged particles like muons (100-200 times heavier than an electron) or entire cascades of particles consisting of electrons and positrons. These charged particles move in water at a speed greater than the speed of light in water, and therefore emit a huge number of photons, which are captured by neutrino telescopes.

Due to the "exotic" features of neutrino detection, neutrino telescopes are not at all like optical or radio telescopes, but rather resemble some installations used in elementary particle physics. Registration is carried out by means of photo-detectors that capture the same Cherenkov radiation. To amplify this radiation, the detectors should also include photoelectronic multipliers-devices that increase the photon flux by 10,000 times.

## 2.2 Underwater neutrino telescopes NT-1000

The Baikal deep-sea neutrino telescope is one of the three largest (along with the already leading data set of the IceCube sub-glacial detector at the South pole and the ANTARES underwater detector in the Mediterranean sea) in terms of its effective area and effective volume of high-energy neutrino detectors.

Deep-sea neutrino telescope NT1000 is designed to solve a wide range of problems of astrophysics, cosmology and physics of elementary particles: search for local neutrino sources, study of diffuse neutrino flux, search for manifestations of dark matter, search magnetic monopoles and other hypothetical particles. Deep-sea telescope of the next generation NT1000 on the lake. Baikal will be an experimental complex aimed at to study natural neutrino fluxes at energies above 10 TeV by detecting Cherenkov radiation from secondary muons and showers generated in neutrino interactions.

The concept of NT1000 is based on a number of fairly obvious requirements for the design and organization of the recording system of the new detector: the maximum possible use of the advantages of installation of the recording system from the ice cover of the lake. Baikal, the capacity of the installation and ensuring its effective operation at the first stages of deployment, the possibility of implementing various options for the layout and density of photo-detectors within a single measurement system. In addition, the principal the requirement is to minimize the time to create a full-scale detector NT1000, which should not exceed 5-6 years.

## 3 Analysis of the data obtained by Monte Carlo

To obtain the characteristics of the effective areas, the data were generated by the Monte Carlo method. This sample was generated with the following parameters:

- physical events are a flow of single isotropic muons;

- 12e+6 events were thrown onto cluster;
- 8.9e+6 events were registered;
- simulation area is 120 x 120 m
- energy spectrum is flat in  $\log_{10}E$
- the noise level is 20 kHz

### 3.1 Angular and energy distribution of events

According to the data obtained, the angular resolution of the registered events was built (Fig. 1).

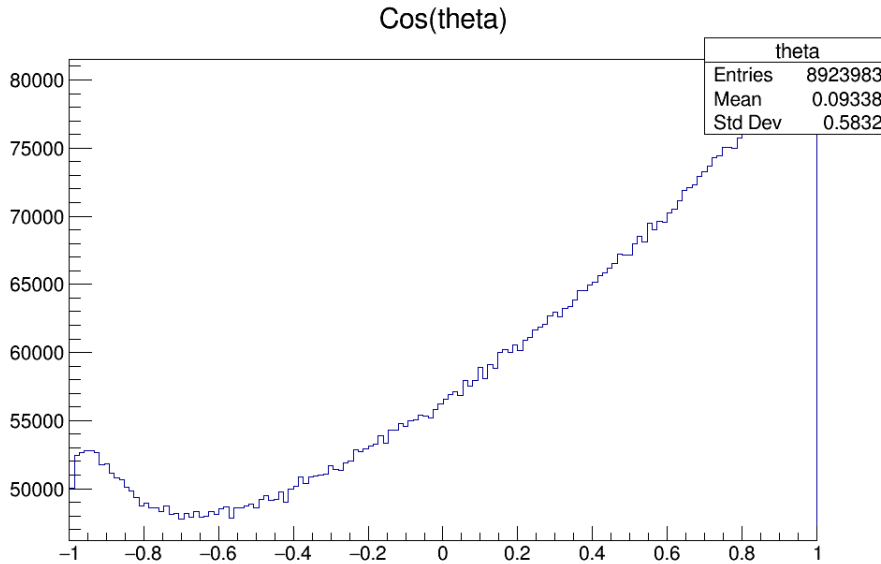


Figure 1: Distribution of muon arrival relative to the Zenith angle.

This distribution tells us that the optical module has a different sensitivity relative to the direction of arrival of the muon. As expected, those areas where photomultiplier's optical modules were more, events was more than any other (Fig. 2).

### 3.2 Triggered strings distribution with separation on energy intervals and without

Registration of flying charged particles occurs by photon registration by photo-electron multipliers. The more photons a charged particle emits, the

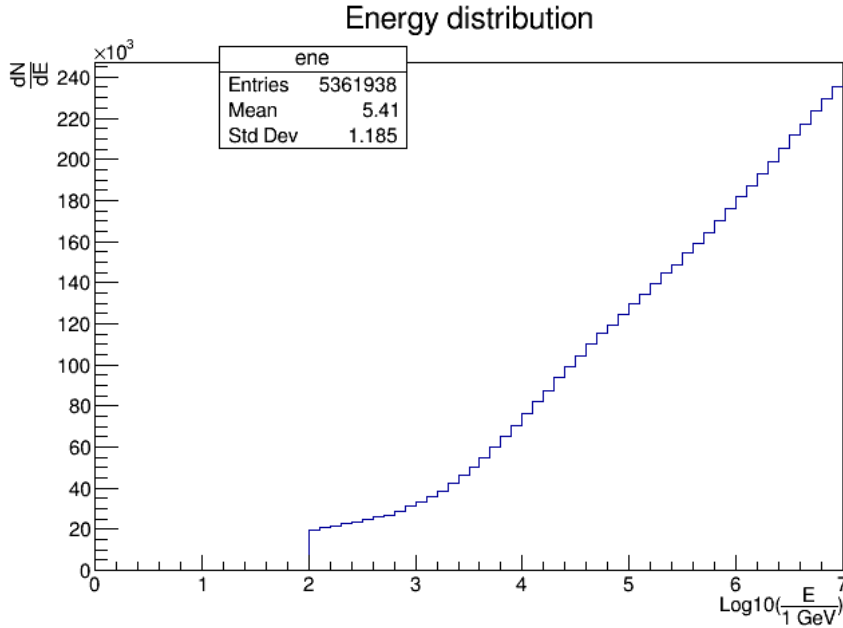


Figure 2: Energy distribution of flown and registered muons in the telescope. The increase in the number of recorded events with the increase in the energy of the event is consistent with the theory, since high-energy particles emit more photons.

more photoelectronic multipliers will be able to register it. Therefore, the more energy of the flying particle, the more information we can get about this particle. There are several criteria that characterize the event, it is:

- Number of hits, made on OM.
- The number of strings, which fell on the photons.

The quality of reconstruction is provided by a large number of hits on different strings. Therefore, it makes sense to look at the number of hits in each event and triggered strings. The distribution of events by the number of triggered strings was built (Fig. 3).

We can see that for 2 triggered strings events with less than 6 hits are the majority. For reconstruction (in the current state of algorithm) 6 hits are sufficient. 5 hits theoretically are also sufficient, however using of 5 hits demands complication of algorithm.

Muon reconstruction begins to restore the tracks, provided that the signal was not less than 3 strings. However, as mentioned above, the restoration of the track can be done if the signal was with 2 strings. Therefore, it is

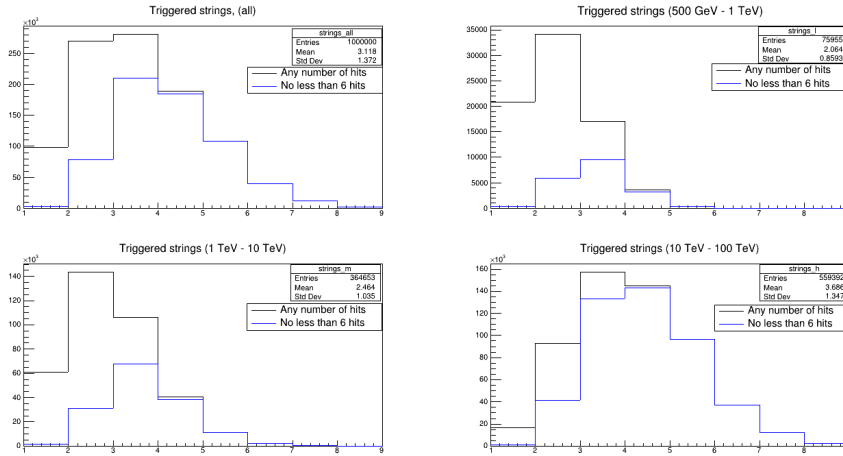


Figure 3: histograms with both  $>6$  hits events and with all events. Histograms are plotted for different energy ranges. The more energy events, the more events with triggered strings. This is consistent with the theory.

interesting to know what increase give events in which the signal was not less than 2 strings. If the increase is significant, it makes sense to improve the reconstruction algorithm.

### 3.3 Zenith angle cosine distribution for $6 \geq 2$ , $6 \geq 3$ and all events with energy separation and percentage ratio

1

Next, we'll see what proportion of all events are events with a given number of hits and triggered strings. For this cosine of zenith angle distribution with separation on type of events was build (Fig. 4).

The ratio of the number of  $6 \geq 2$  and  $6 \geq 3$  events to the total number of events is:

- 63,58 % and 55,75 % respectively. The increase in the number of registered events is 7,83 %.

Also, cosine of zenith angle distribution with separation on type of events for any energy range was build (Fig. 5).

The ratio of the number of  $6/2$  and  $6/3$  events to the total number of events is:

---

<sup>1</sup>This designation denotes physical events with 6 or more hits and 2 (or 3) and more triggered strings

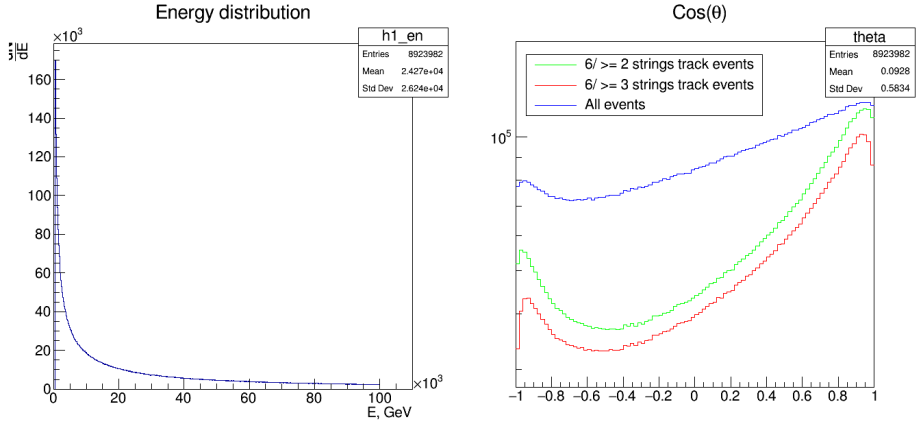


Figure 4: Histogram of cosine of zenith angle distribution for all events and energy distribution.

- 25,01 % and 17,20 % in the energy range (500 GeV - 1 TeV). The increase in the number of registered events is 7,81 %.
- 41,27 % and 32,82 % in the energy range (1 TeV - 10 TeV). The increase in the number of registered events is 8,45 %.
- 83,35 % and 75,91 % in the energy range (10 TeV - 10 TeV). The increase in the number of registered events is 7,44 %.

## 4 Analysis of NT-1000 cluster transparency for low-energy muons

It is well known that NT-1000 is not transparent for muons with energy greater than 10 TeV. However, it isn't checked if telescope has insensitive zones for 0.5-1 TeV muons.

### 4.1 Search for insensitive zones candidates

First of all it is reasonable to look at a cluster of NT-1000 in the scope of geometry. A cluster has two candidates for such zones. Up-going and down-going muons can be missed, but only the second option was examine. It is insensitive zones in horizontal-plane. Geometrical searches was provide with picture (Fig. 6).

This is the top-view(XOY plane) on the NT-1000 cluster. There are 14 best projections on horizontal plane from trajectories of muons, which are

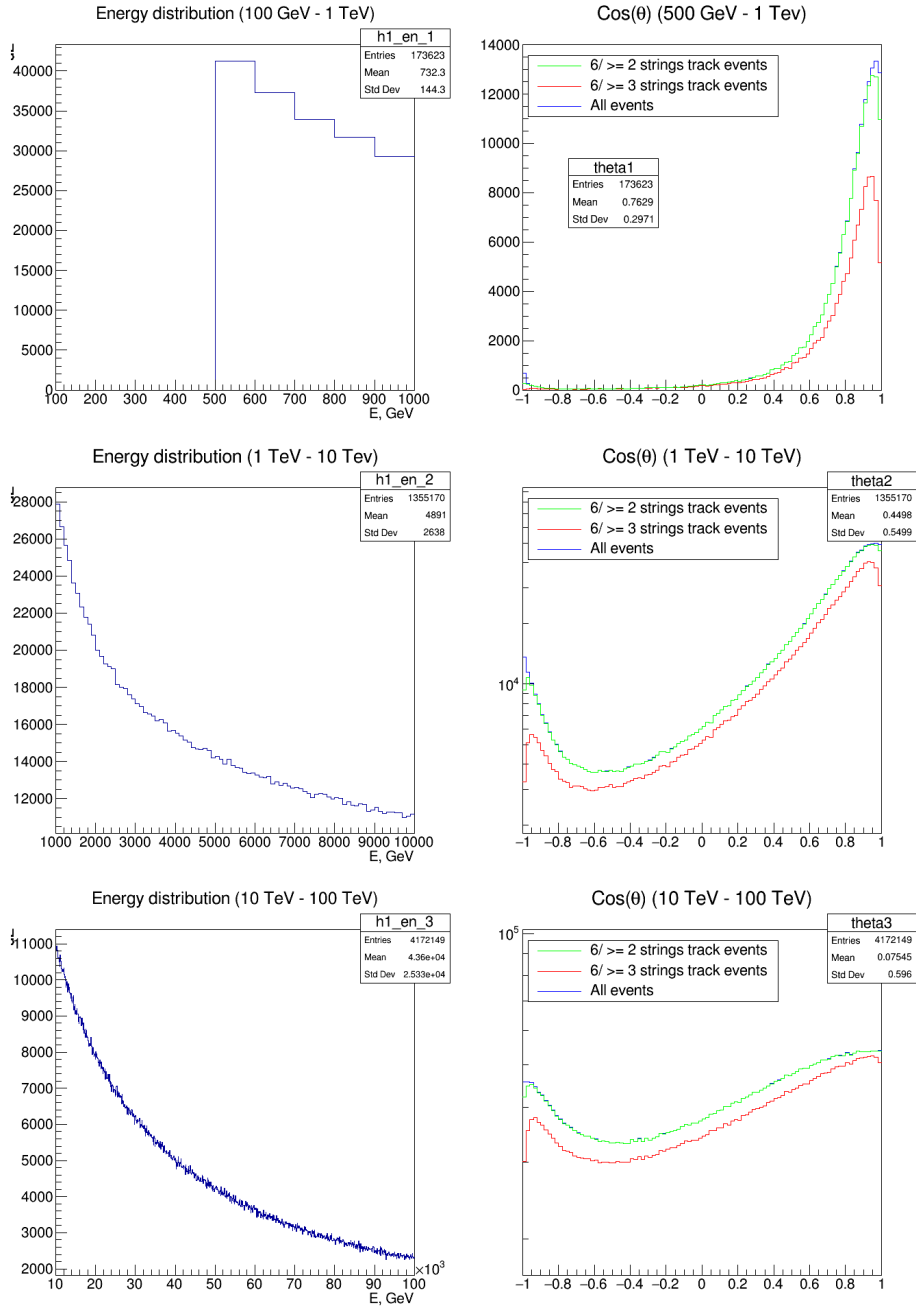


Figure 5: Histogram of cosine of zenith angle distribution for all events and energy distribution for energy range [500 GeV - 1 TeV], [1 TeV - 10 TeV], [10 TeV - 100 TeV].

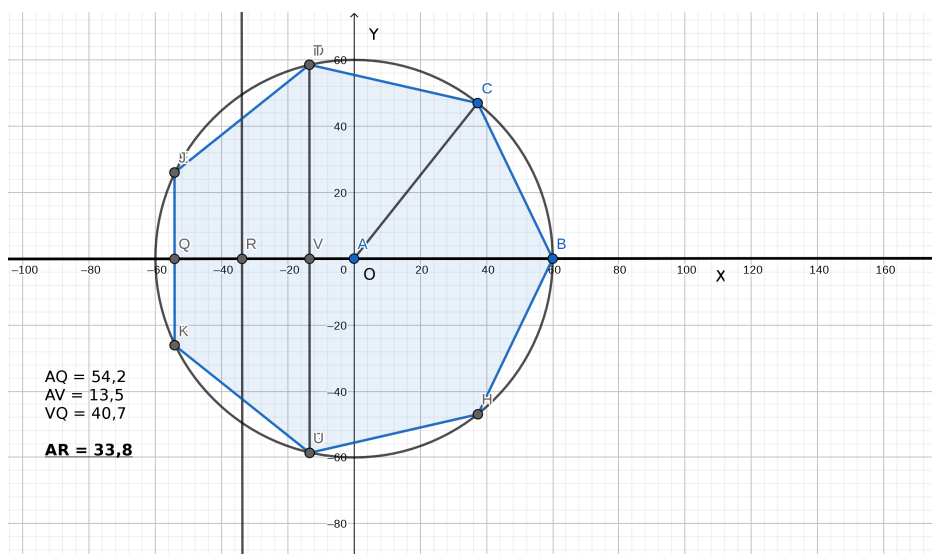


Figure 6: Schematic representation of a cluster of a neutrino telescope.

candidates to be a insensitive zone. Two for each side of the heptagon(they are both on the same line, but have different directions). It is to see on the picture, if the effective range of muon detection is around 17m around it's trajectory, there are small corridor for same-azimuth trajectories to stay unregistered ( around 6.7 meters).

A script was made, which could help to understand if NT-1000 has such zones or not.

## 4.2 Coordinates transformation

The histograms below will represent distributions of events for azimuth angle and horizontal offset of muon trajectory. Let's explain what "horizontal offset" is. Muon trajectory in MC-data is represented as azimuth and zenith angle and a point on the trajectory which also lies on the plane perpendicular to muon trajectory. Muons with the same angles are distributed through this plane. We can transform joint points of trajectories and the plane from Cartesian 3d coordinates to Cartesian 2d coordinates on the plane. Only horizontal offsets make sense for geometrical transparency in such plane.

It take to get the direction at the intersection of planes XOY and the plane with normal vector  $\vec{n}$ .

$$\begin{cases} (\vec{n}, \vec{r}) = 0 \\ z = 0 \\ \vec{n} = (\cos \phi \sin \theta, \sin \phi \sin \theta, \cos \theta) \end{cases}$$

The equation of the line at the intersection was got by solving.

$$\begin{cases} n_x x + n_y y = 0 \\ z = 0 \end{cases}$$

$\vec{n}_v$  is a normalized vector with chosen orientation on the line of planes intersection.

$$\vec{n}_v = \frac{1}{\sqrt{n_x^2 + n_y^2}}(n_y, -n_x, 0)$$

Then horizontal(in the XOY plane) offset of muon trajectory was got and built 2D histograms.

Horizontal offset  $v$  :

$$v = (\vec{r}, \vec{n}_v);$$

These histograms show the distribution of the number of events relative to their horizontal displacement and azimuthal angles in the energy range less than 700 GeV (Fig. 7, 8)

## 5 Effective and geometrical areas of a NT-1000 cluster

The effective area of the cluster shows the efficiency of particle registration in the cluster. This area is equal to the area of a flat figure, the center of which is in the center of the cluster and it is perpendicular to the track of the flying particle. If a particle enters this area, it will be registered.

### 5.1 Geometrical projection

It is interesting to compare the effective area with the geometric projection on a plane perpendicular to the track of the incident particle. Therefore, a graph of the cluster projection dependence on the angle of view, which coincides with the angle of theta, was built. To simplify the calculations, the cluster shape was taken as a cylinder (Fig. 9).

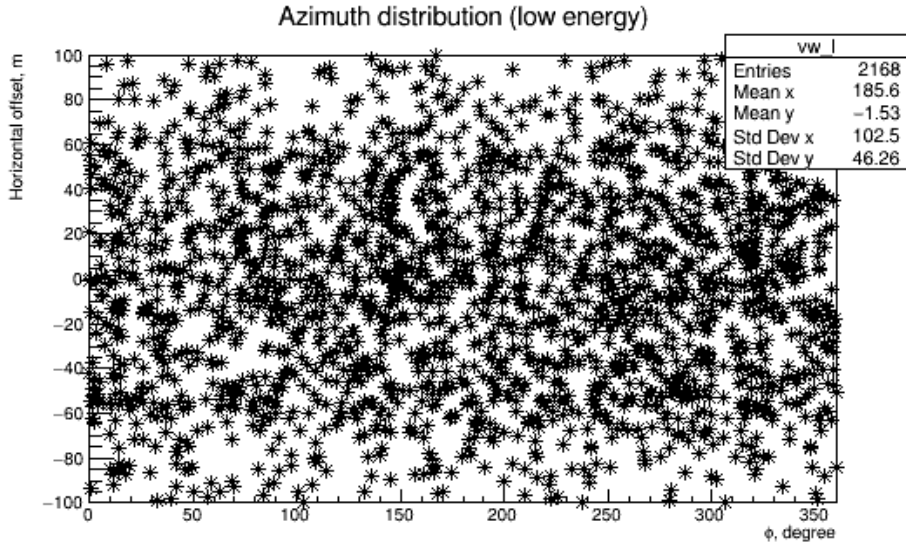


Figure 7: Horizontal displacement of events in a cluster  
Azimuth distribution with  $v = 33.8 \pm 5$  (low energy)

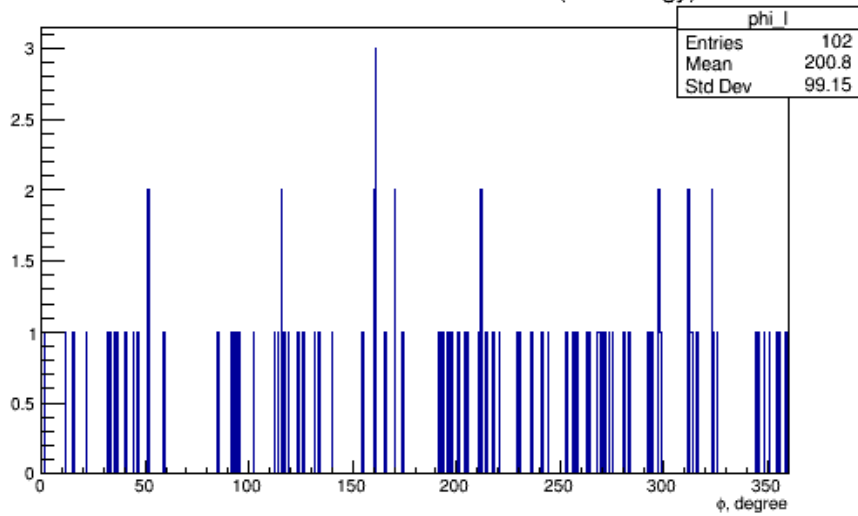


Figure 8: The azimuth distribution of events in a cluster

## 5.2 Calculation of effective areas

Effective area can be computed through next formula:

$$S_{\text{eff}} = \frac{N_{\text{det}}}{N_0} S_{\text{MC}}, \text{ where}$$

$N_{\text{det}}$  - Number of registered particles,  $N_0$  - The number of particles,

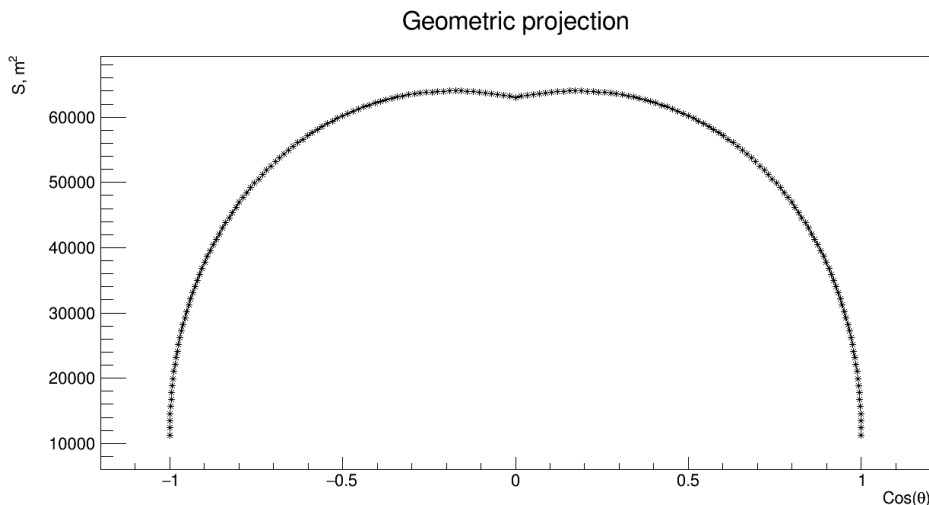


Figure 9: The dependence of the geometric projection of the cluster on the cosine angle of view

thrown at the cluster,  $S_{MC}$  - The area where the particles were thrown.

Consider the dependence of the effective area of the angle at which the particles fly and the dependence on the energy of the particles. In the first case, the effective area is calculated using the following formula:

$$S_{\text{eff}}(\theta) = \frac{N_{\text{det}}(\theta)}{N_0(\theta)} S_{MC}$$

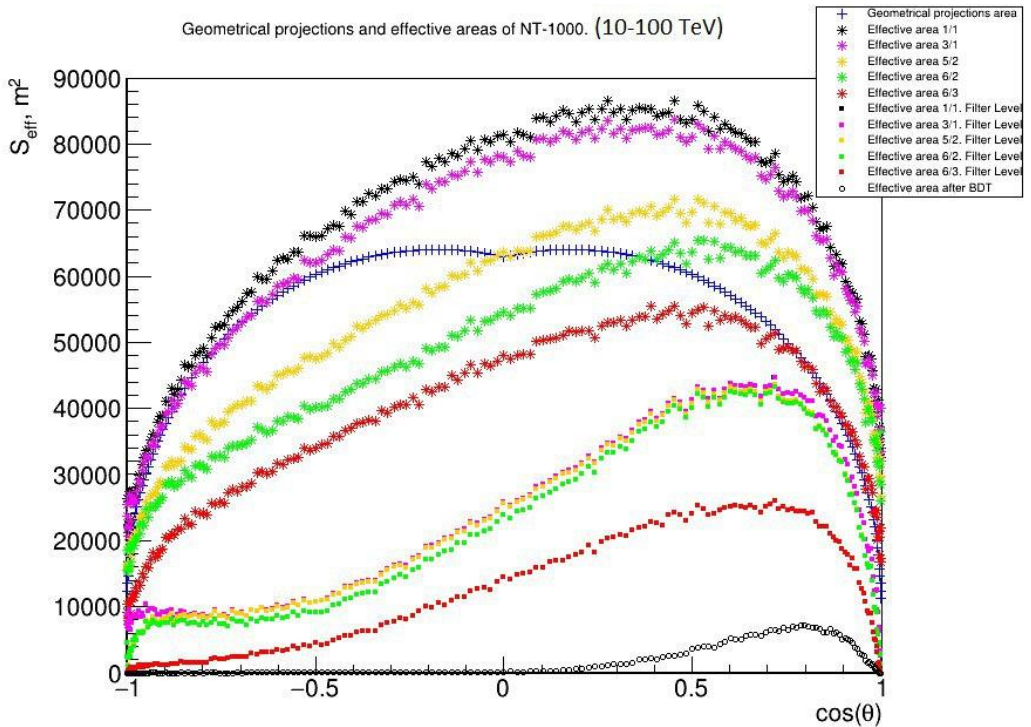
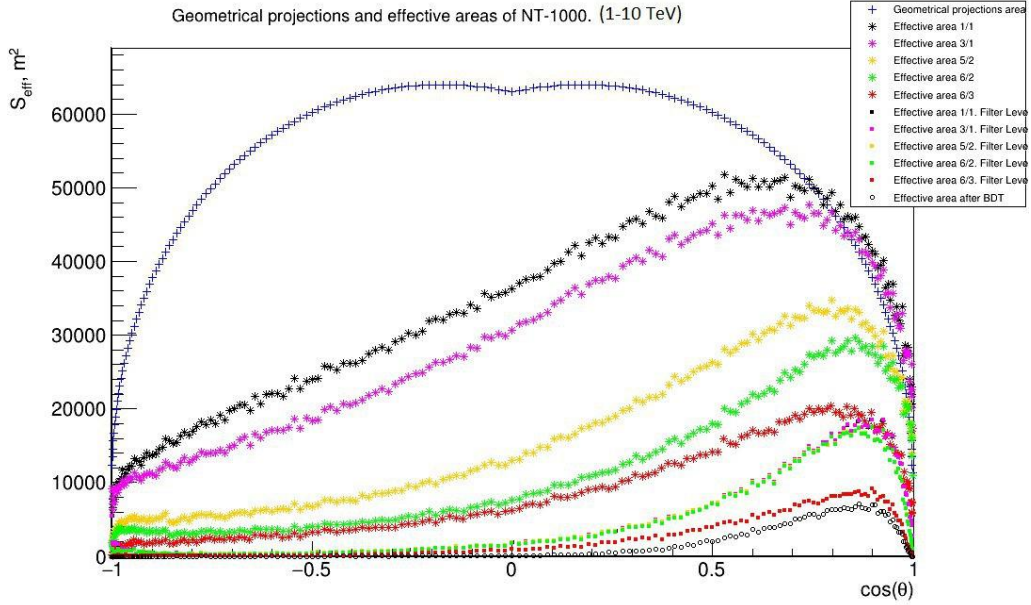
$N_{\text{det}}(\theta)$  - Number of registered particles, flying at an angle theta. Since the sampling parameters are such that the events are thrown on the cluster isotropically, and their energy spectrum is flat in log,  $N_0(\theta)$  is considered by the formula:

$$N_0(\theta) = \frac{N_{\text{all}}}{4\pi} \int_0^{2\pi} d\phi \int_{\theta}^{\theta+1^\circ} \sin(\theta) d\theta \frac{\int_{E1}^{E2} d(\lg(E))}{\Delta E}$$

We have made separation  $\theta \in [0^\circ; 180^\circ]$  by 1 degree. So, we must consider amount of thrown muons as product of number of all muons and of part of solid angle in every interval  $\theta \in [\theta_0, \theta_0+1^\circ]$ . There is a possibility to calculate effective area in selected energy interval  $[E1, E2]$ .

As a result, effective areas were constructed depending on the cosine of the Zenith angle for different energy ranges and depending on the energies for different ranges of Zenith angles (Fig. 10). The graphs show that the effective areas are larger for the Zenith angles of 45 degrees. As the Zenith angle increases, the effective area decreases. This is due to the fact that the

optical modules have a high sensitivity of photon registration from below. And on top of the sensitivity of the optical modules is worse. Therefore, the obtained dependences are consistent with the theory.



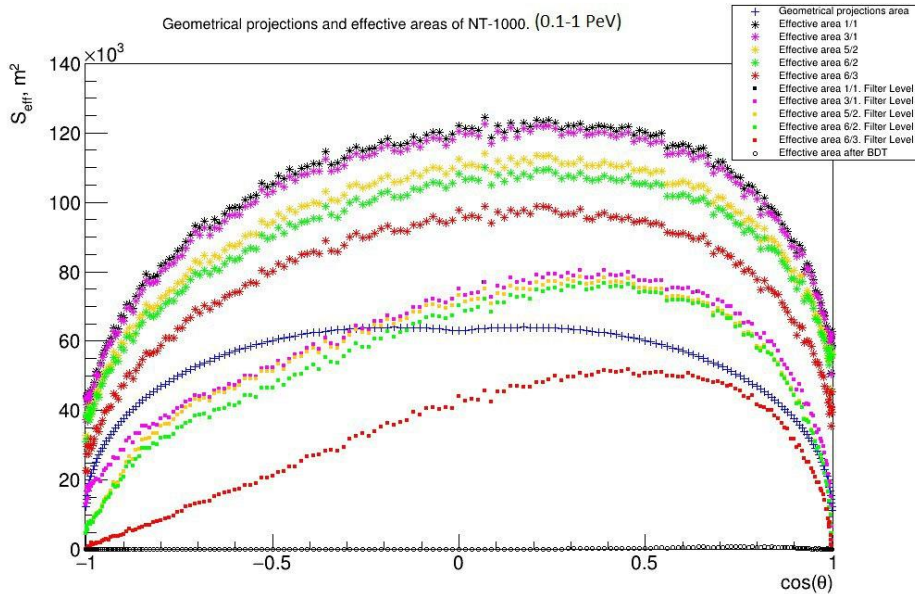


Figure 10: Dependence of the effective area on the cosine of the Zenith angle for energy ranges  $[1, 10(\text{TeV})]$ ,  $[10, 100(\text{TeV})]$  and  $[0.1, 1(\text{PeV})]$

Also the dependence of the effective area on the particle energy for different zenith angles was constructed (Fig. 11). The graphs show that the effective areas increase with the particle energy. The more energy particles the more light it emits. Accordingly, particle registration is better and more thrown particles will be registered. Therefore, the effective area should increase with increasing particle energy.

## 6 Conclusion

The graphs show that the highest efficiency of registration is achieved at small zenith angles  $[30^\circ, 60^\circ]$  and at high energies.

The effective areas are obtained using data obtained by the Monte Carlo method. The obtained characteristics are consistent with the theory.

It is also worth noting that the effective area of the cluster grows with increasing energy. When the energy of the particles is 4.5 TeV, this area becomes equal to the geometric area of the cluster. In the energy range  $[1, 10]$  TeV effective area exceeds the geometric area at the cosine of the Zenith angle from 0 to 1. At high energies, the effective area almost everywhere exceeds the geometric one. However, in the Zenith angle ranges from  $0^\circ$  to  $90^\circ$ , the effective area is higher than in the other angle range. This is due to the fact

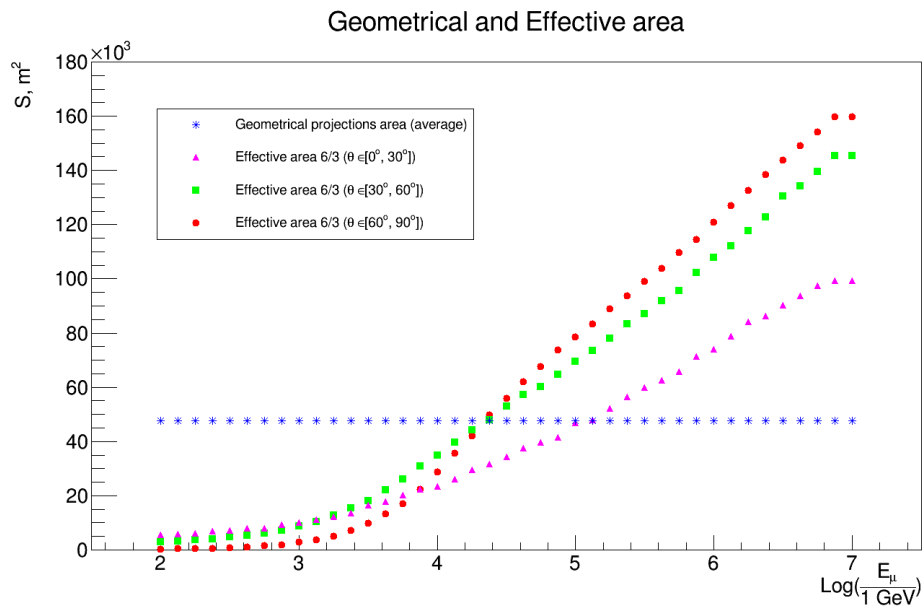


Figure 11: The dependence of effective area on the energy of the particle for a range of angles  $[0^\circ, 30^\circ]$ ,  $[30^\circ, 60^\circ]$  and  $[60^\circ, 90^\circ]$

that the optical modules have a greater sensitivity of registration from the bottom than from the top.